

# The Role of *Escherichia coliform* in the Biomineralization of Calcium Oxalate Crystals

Long Chen,<sup>[a]</sup> Yuhua Shen,<sup>\*,[a]</sup> Rong Jia,<sup>[b]</sup> Anjian Xie,<sup>\*,[a,c]</sup> Bei Huang,<sup>[b]</sup> Xiaobin Cheng,<sup>[b]</sup> Qingfeng Zhang,<sup>[a]</sup> and Ruiyong Guo<sup>[b]</sup>

**Keywords:** Urolithiasis / *Escherichia coliform* / Calcium oxalate / Nucleation and growth / Biomineralization

The influence of the common bacterium *Escherichia coliform* (*E. coli*) on the nucleation and growth of calcium oxalate (CaOxa) in aqueous solution is studied in order to determine its role in the biomineralization of urinary stones. The results show that CaOxa crystals obtained in the presence of *E. coli* transform more quickly from calcium oxalate dihydrate (COD) into calcium oxalate monohydrate (COM), and they become even larger, than in the absence of the bacterium. On decreasing the concentration of chemical reagents, in other words increasing the ratio bacterium/CaOxa, except for the more rapid phase transition from COD to COM, the CaOxa particles obtained become larger and more regular with a hexagonal morphology. This suggests that *E. coli* accelerates the crystallization of COM, which is the most stable crystal phase of CaOxa and the major component of urinary stones. Transmission electron microscopy (TEM) images, electron diffraction (ED) patterns, and Fourier-transform IR (FTIR) spectra show that the biomineralization process of

CaOxa crystals takes place both inside and outside the bacterium, which implies that it is induced by both intracellular biomolecules and the bioorganic secretions of the bacteria. Sodium dodecyl sulfate polyacrylamide gel electrophoresis (SDS-PAGE) data and UV/Vis spectra show that the proteins bound to the crystal surface with a molecular weight of around 26.5 kDa have tyrosine, tryptophan, or phenylalanine residues. The zeta potential and FTIR spectra are used to investigate the mineralization mechanism of CaOxa with *E. coli* and show that, the negatively charged biomolecules inside and outside the bacterium interact with  $\text{Ca}^{2+}$  ions to provide nucleation sites and then act as modifiers to induce the nucleation, growth, and aggregation of COM crystals. Therefore, we infer that *E. coli* mineralizes calcium oxalate and plays a role in the formation of urinary stones.

(© Wiley-VCH Verlag GmbH & Co. KGaA, 69451 Weinheim, Germany, 2007)

## Introduction

Urolithiasis is a common disease affecting millions throughout the world that remains a serious health concern due to its severe symptoms, such as great pain and urinary-tract obstruction and infection. At present, stones are mainly treated by surgery or extracorporeal shock wave lithotripsy followed by prolonged antibiotic treatment and oral citrate, although these remedies are unsatisfactory because of a high rate of recurrence. No effective drugs or treatment methods for this stubborn disease are currently available, therefore many studies on the mechanism of stone formation have been performed in recent years in the search for such treatments and methods. A number of questions still remain, however, regarding the factors that promote

and inhibit stone formation, some of which are somewhat controversial.<sup>[1]</sup>

A urinary stone is a product of abnormal biomineralization whose principal mineral component is calcium oxalate monohydrate (COM),<sup>[2,3]</sup> which is the thermodynamically most stable phase of CaOxa. The other two phases of CaOxa, namely calcium oxalate trihydrate (COT) and calcium oxalate dihydrate (COD), rarely form stones as they are unstable and are more easily excreted in the urine than COM. In these stones, inorganic crystals are always mixed with organic matrices such as lipids, carbohydrates, and proteinaceous materials, and studies have shown that, although these organic materials account for only about 2% of the total mass, they play a very important role in the stone-formation process.<sup>[4,5]</sup> To better understand the role of organic matrices in urinary stone formation, Langmuir monolayers,<sup>[6–12]</sup> vesicles,<sup>[13]</sup> biomolecules,<sup>[14]</sup> etc., have all been used to induce the nucleation and growth of COM crystals. Our groups have recently studied the crystal growth of CaOxa in a reverse microemulsion of *p*-octyl polyethylene glycol phenyl ether (OP)/isooctyl alcohol (IOA)/cyclohexane/water containing different kinds of amino acids, and found that the type of amino acid, the pH, and surfactant can all influence the formation of CaOxa

[a] School of Chemistry and Chemical Engineering, Anhui University, Hefei 230039, P. R. China  
Fax: +86-551-510-7342  
E-mail: s\_yuhua@163.com  
anjx@163.com

[b] School of Life Science, Anhui University, Hefei 230039, P. R. China

[c] Key Laboratory of Environment-Friendly Polymer Materials of Anhui Province, Hefei 230039, P. R. China

crystals.<sup>[15]</sup> We have also investigated crystal growth of CaOxa induced by octadecanoic acid/octadecylamine monolayers influenced by different concentrations of human serum albumin, and obtained different morphologies of CaOxa crystals with three kinds of phases.<sup>[16]</sup> We have also successfully inhibited the phase transition from COT to COM with 1,2-bis(*O*-aminophenoxy)ethane-*N,N,N,N*-tetraacetic acid.<sup>[16]</sup>

Some microorganisms, especially nanobacteria, have been reported to be involved in the formation of urinary stones. Nanobacteria are very tiny bacteria that range from 80–500 nm in size which have been isolated from renal stones<sup>[17,18]</sup> and have been shown to mineralize calcium and phosphate even under physiological conditions.<sup>[19,20]</sup> Cuerpo et al., for example, have found that when these bacteria are injected intravenously they accumulate in the kidney and produce apatite,<sup>[21,22]</sup> which suggests that the kidney is a preferred site for mineralization by these tiny bacteria, and Shiekh et al. have investigated the effects of intravenous administration of nanobacteria on the kidneys of Wistar rats and have found evidence for their inflammatory infiltration and accumulation in the cortex; in addition, small uniform renal calcification was seen on the surface of renal tubules.<sup>[23]</sup> These studies have therefore shown that nanobacteria may act as biomineralization centers for the initiation of kidney stones and play a contributory role in urolithiasis. Instead of promoting the formation of stone, oxalate-eating bacteria such as *Oxalobacter formigenes* can degrade oxalate and prevent the occurrence of CaOxa urolithiasis.<sup>[24,25]</sup>

The common bacterium *Escherichia coli* (*E. coli*) is often found in urinary stones and it could damage the protective anti-adhesive GAG layer and cause crystal retention or alter urine composition in such a way that favors stone formation.<sup>[26,27]</sup> It has also been found that *E. coli* plays an important role in urinary-tract infections.<sup>[28]</sup> However, to date, there is no report of its true role in the biomineralization of urinary stones. In the present study, we report that *E. coli* can induce the nucleation, growth, and aggregation of CaOxa by biomolecules internally or externally and promote the formation of COM with a regular morphology, which suggests that it plays a contributory role in the biomineralization of urinary stones. This may help our further understanding of the stone-formation mechanism and lead to a method for the prevention and treatment of urolithiasis. In addition, it is also significant for the synthesis of inorganic materials with different morphologies.

## Results and Discussion

SEM images of CaOxa particles obtained after an aging time of 5 h in the absence and presence of *E. coli* are shown in Figure 1; the corresponding XRD patterns are shown in Figure 2. It can clearly be seen that the CaOxa particles obtained under these two conditions have different sizes and crystal phases. Without the bacterium, quasi-hexagonal or irregular CaOxa particles with an average diagonal of about

150 nm (shown in Figure 1a) are obtained. The corresponding XRD patterns (shown in Figure 2a) display diffraction peaks at 14.22°, 15.08°, 19.90°, 24.44°, 30.20°, 31.66°, and 32.02°, which can be indexed to the (*hkl*) indices (200), (211), and (411) of a COD phase (JCPDS card number 17-541), and the ( $\bar{1}01$ ), (020), ( $\bar{2}02$ ), and (121) indices of a COM phase (JCPDS card number 20-231), respectively. This indicates that the crystals obtained are a mixture of COM and COD. Figure 1b shows that hexagonal or rhombic particles with an average diagonal of about 300 nm are obtained in the presence of *E. coli* (0.5 wt.-%) that are larger than those formed without the bacterium. The XRD patterns (Figure 2b) show that they are all COM. These results imply that *E. coli* promotes the crystallization of COM and influences the size and morphology of the product.

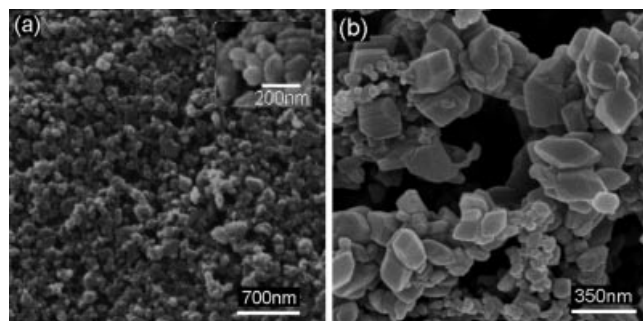


Figure 1. SEM images of CaOxa precipitates obtained in different systems after 5 h of reaction: (a) without *E. coli*, (b) with *E. coli* (0.5 wt.-%). The inset in (a) is a magnification.

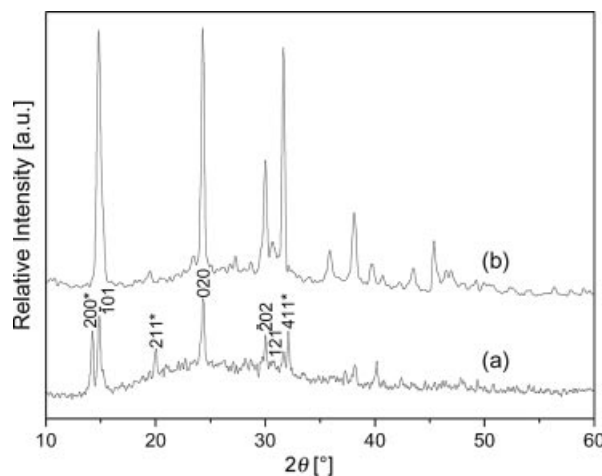


Figure 2. XRD patterns of CaOxa precipitates obtained in different systems after 5 h of reaction: (a) without *E. coli*, (b) with *E. coli* (0.5 wt.-%). The peaks of COD are labeled with an asterisk.

In order to investigate the influence of aging time and the ratio bacterium/chemical reagents on the formation of CaOxa, SEM images (Figure 3) and XRD patterns (Figure 4) of the products formed in two systems at different reaction times were recorded. At a CaOxa concentration of  $2.5 \times 10^{-2}$  M the mass ratio bacteria/CaOxa is 1.56:1 (*E. coli*: 0.5 wt.-%) and the morphologies of CaOxa particles obtained transform from predominantly bipyramidal to predominantly hexagonal, although the sizes show no obvious

changes (range from 100–600 nm) after aging for between 5 min and 3 d (shown in Figure 3a–d). The corresponding XRD patterns show that the CaOxa obtained has two phases including COD and COM (shown in Figure 4a–d). If  $I_D$  and  $I_M$  are defined as the intensity of the characteristic diffraction peaks of COD (200) and COM ( $\bar{1}01$ ), the percentage of COD in the mixture can be calculated from the equation  $\% \text{COD} = I_D / (I_M + I_D)$ .<sup>[29]</sup> With aging times of 5 min, 30 min, 3 h, and 3 d, the percentage of COD in the products is 55.6%, 52.7%, 26.5%, and 0.02%, respectively. This clearly shows that the amount of COD in the crystals decreases gradually and almost disappears with an increase of aging time, which suggests that thermodynamically unstable COD changed into stable COM with time.

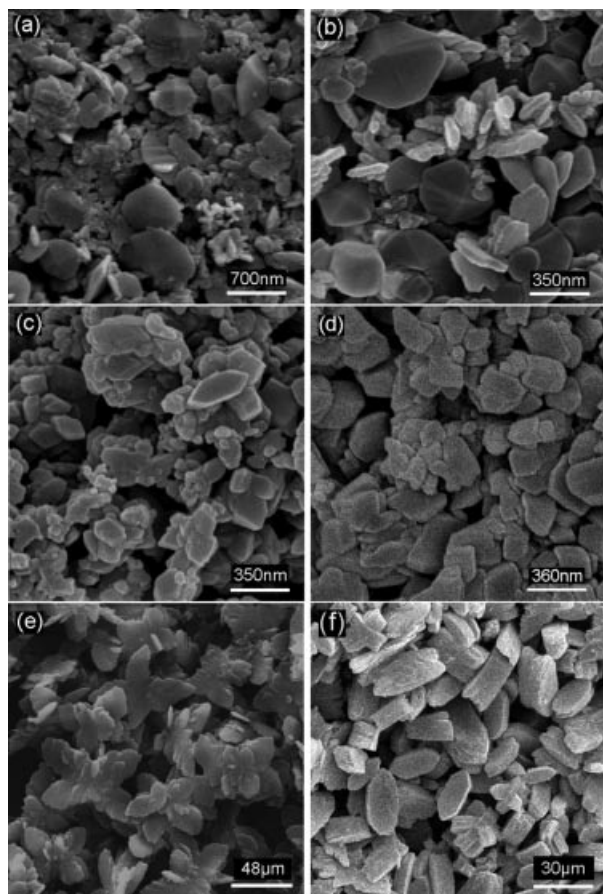


Figure 3. SEM images of CaOxa precipitates obtained in two systems at different reaction times: (a)–(d) concentration of CaOxa of  $2.5 \times 10^{-2}$  M with aging times of 5 min, 30 min, 3 h, and 3 d, respectively, with 0.5 wt.-% *E. coli*; (e), (f) concentration of CaOxa of  $2.5 \times 10^{-3}$  M and aging times of 3 h and 3 d, respectively, with 0.5 wt.-% *E. coli*.

Decreasing the concentration of CaOxa to  $2.5 \times 10^{-3}$  M increased the mass ratio bacteria/CaOxa (15.6:1) and the sizes and morphologies of the CaOxa particles obtained also changed. It can be seen from Figure 3e, taken after 3 h, that flower-like CaOxa particles were obtained. Every “petal” of the “flower” is quasi-hexagonal with a mean diagonal of around 30  $\mu\text{m}$ . The corresponding XRD patterns show that they are all COM crystals (Figure 4e). To the

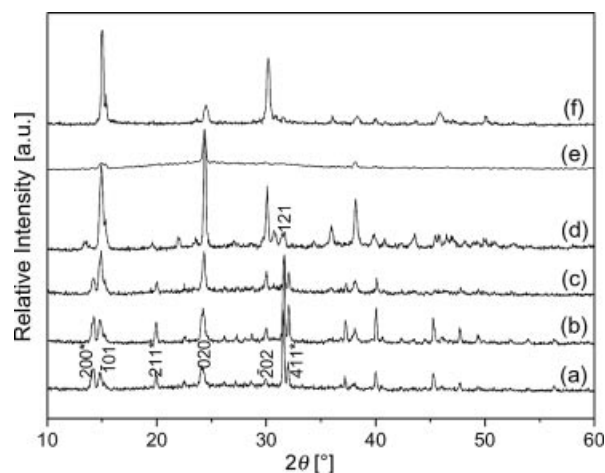


Figure 4. XRD patterns of CaOxa precipitates obtained in two systems at different reaction times: (a)–(d) concentration of CaOxa of  $2.5 \times 10^{-2}$  M with aging times of 5 min, 30 min, 3 h, and 3 d, respectively, with 0.5 wt.-% *E. coli*; (e), (f) concentration of CaOxa of  $2.5 \times 10^{-3}$  M and aging times of 3 h and 3 d, respectively, with 0.5 wt.-% *E. coli*. The peaks labeled with an asterisk correspond to COD.

best of our knowledge the general morphology of COM is hexagonal, therefore the “flowers” probably form due to the aggregation of several single hexagonal COM particles. This suggests that *E. coli* influences the growth and aggregation of CaOxa. When the aging time was increased to 3 d mainly hexagonal CaOxa particles with an average diagonal of around 30  $\mu\text{m}$  were obtained (Figure 3f). Compared with those formed after 3 h, these particles are isolated with no apparent change in size. The XRD results show that they are also COM (Figure 4f), although the strongest diffraction peak is ( $\bar{1}01$ ) instead of (020), which implies that the bacterium (*E. coli*) influences the crystallization process.

It can be seen from the above results that the CaOxa particles obtained become larger, more regular, and aggregate more easily with an increase in the bacteria/CaOxa ratio and that, at the same aging time (3 h), the phase transition from COD to COM is more rapid. This further suggests that *E. coli* accelerates the crystallization of COM and makes the particles become larger. Larger COM particles form urinary stones more easily because they are more difficult to excrete, therefore we can speculate that *E. coli* plays an important role in the biom mineralization process of urinary stones. In addition, it can also be speculated from the above results that a higher concentration of CaOxa does not always result in a risk of urinary stones.

TEM images of the products obtained by drying the reacting solution containing  $2.5 \times 10^{-3}$  M CaOxa and 0.5 wt.-% *E. coli* after aging for 12 h were recorded in order to explore the details of nucleation and growth of COM induced by *E. coli* (see Figure 5). It can clearly be seen that there are many uniform spindle-shaped particles in the CaOxa-centered area (Figure 5a), which were proved by their electron diffraction (ED) pattern (Figure 5c) to be COM crystals. When examined carefully, these crystals are found to be enclosed by light shells. We infer that the light



materials on the crystal surface are the bioorganic secretions of the bacterium. In addition, many light, rod-like bacteria (*E. coli*) can be seen in the bacteria-centered area (Figure 5b). The darker parts seen in the bodies of some bacteria were shown from their ED patterns (Figure 5d) to be COM crystals. This suggests that  $\text{Ca}^{2+}$  and  $\text{C}_2\text{O}_4^{2-}$  ions can enter into the cells of the bacteria and form COM crystals due to inducement by intracellular biomolecules. In other words, the bacteria can control the nucleation and growth of COM crystals in their interior. In order to confirm the TEM results, the FTIR spectrum of CaOxa crystals obtained from the solution after the same reaction time was determined (Figure 6). It can be seen from this spectrum that the symmetric and antisymmetric oxalate  $\text{C}=\text{O}$  stretching bands are located at 1618 and 1321  $\text{cm}^{-1}$ , respectively. Very importantly, the band located at 1640  $\text{cm}^{-1}$  (amide I) shows that the CaOxa obtained contains *E. coli* proteins. The surface-bound proteins released from the COM crystals grown in the presence of *E. coli* were removed by treatment with NaOCl and analyzed by 10% sodium dodecyl sulfate polyacrylamide gel electrophoresis (SDS-PAGE) at pH = 8.2. The data show that the surface-bound proteins have a molecular weight of about 26.5 kDa (lane 2, Figure 7a). The UV/Vis spectrum of the surface-bound proteins is shown in Figure 7b. The peak at 210 nm was assigned to the strong absorption of the peptide bonds of the protein in the extract, which arises from an  $n-\pi^*$  transition of the  $\text{C}=\text{O}$  group. The absorption at 280 nm is due to the  $\pi-\pi^*$  transition of the tyrosine, tryptophan, or phenylalanine residues of the proteins. Two enzymes in urine, namely sialidase and urokinase, are thought to play a role in urolithiasis. Sialidase is responsible for the conversion of urinary mucosubstances into mineralizable matrix and urokinase regulates the urinary uromucoid concentration. du Toit et al.<sup>[30]</sup> have found that *E. coli* can inhibit urokinase and stimulate sialidase activity, which leads to the formation of a mineralizable stone matrix. They also suggested that *E. coli* might cause urolithiasis by producing matrix substances that increase crystal adherence to the epithelium.<sup>[31]</sup> The average concentration of *E. coli* in the urine of patients with a urinary tract infection or urolithiasis is about  $10^6$  cells/mL,<sup>[32,33]</sup> which is very close to the experimental levels found by du Toit et al.<sup>[30]</sup> It can be speculated that the CaOxa surface-bound proteins with a molecular weight of about 26.5 kDa are probably the urokinase inhibitor and sialidase stimulator synthesized by *E. coli* during incubation.<sup>[30]</sup> Except for altering the excretion of the two enzymes, these proteins could also act as matrices for stone formation. Further investigations are in progress to determine the sequences of the proteins and the nature of the interaction of the proteins with the different crystallographic faces of CaOxa crystals. Taken together, these results suggest that the bacteria and their secretions participate in the crystallization of CaOxa, which means that *E. coli* can mineralize calcium and oxalate both intracellularly and with their bioorganic secretions. Previous studies have shown that nanobacteria can mineralize calcium and phosphate and act as crystallization centers during the formation

of urinary stones,<sup>[21–23]</sup> therefore we speculate that *E. coli* probably also acts as a nucleus in the biomineralization of urinary stones.

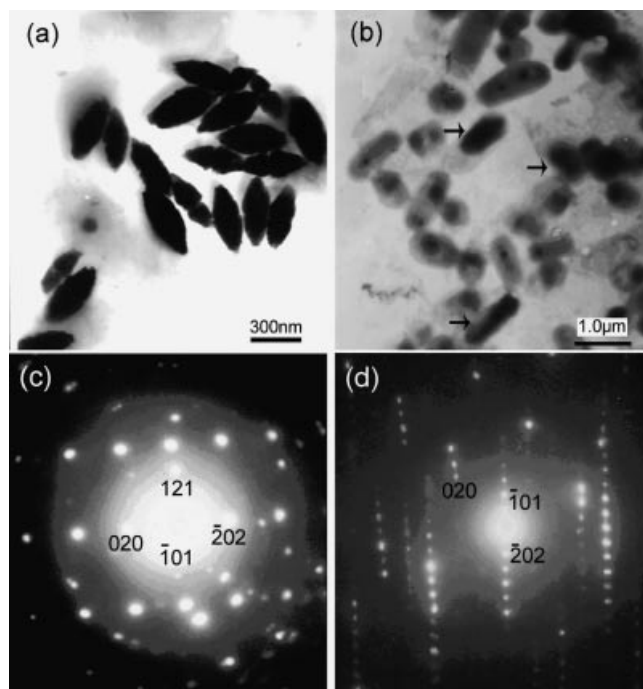


Figure 5. TEM images of the products obtained by drying the reaction solution containing  $2.5 \times 10^{-3}$  M CaOxa and 0.5 wt.-% *E. coli* after aging for 12 h [(a): CaOxa-centered area; (b): bacteria-centered area] and electron-diffraction (ED) patterns of the crystals obtained [(c): CaOxa-centered area; (d): bacteria-centered area]. The arrows in (b) point to CaOxa crystals grown in cells of *E. coli*.

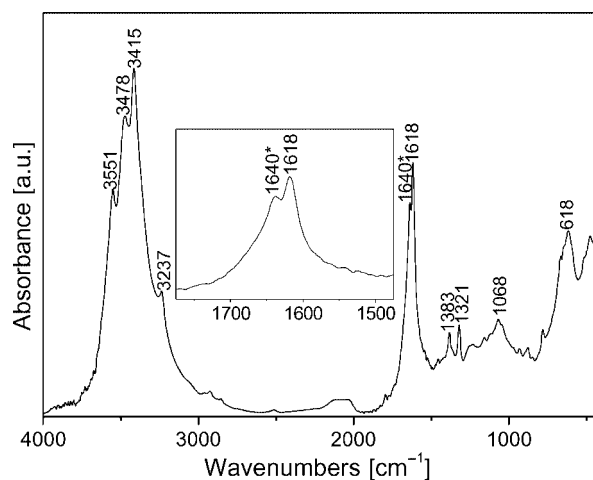


Figure 6. FTIR spectrum of CaOxa particles obtained from the reaction solution containing  $2.5 \times 10^{-3}$  M CaOxa and 0.5 wt.-% *E. coli* after aging for 12 h. The inset shows the magnification of the bands located at 1618 and 1640  $\text{cm}^{-1}$ . The peak labeled with an asterisk is the amide I band of the *E. coli* proteins.

To the best of our knowledge, the cell walls of *E. coli* are composed of lipopolysaccharide and peptidoglycan, which is a polymer of glucide and protein with a polysaccharide structure, 30% of whose subunits (*N*-acetylglucosamines and *N*-acetylmuramic acids) interlace together to form a

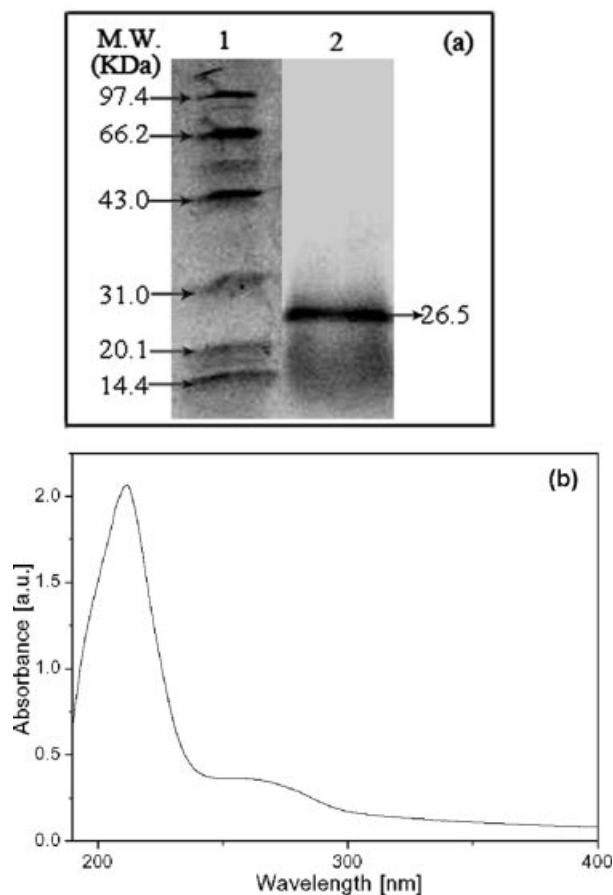


Figure 7. (a) SDS-PAGE data showing the proteins that were originally bound to the surface of the COM crystals grown in the presence of *E. coli*. Lane 1 shows standard protein molecular weight markers with the corresponding molecular weights, in kDa, indicated by arrows. Lane 2 corresponds to the protein bands in the *E. coli* secretions obtained by treatment of COM crystals grown in the presence of *E. coli* with NaOCl. (b) UV/Vis spectrum of the proteins obtained by treatment of COM crystals grown in the presence of *E. coli* with NaOCl.

relatively loose structure with many bare electronegative groups, which could attract and combine with  $\text{Ca}^{2+}$  ions to provide nucleation sites. In addition, proteins and other biomolecules present in the cell could also interact with  $\text{Ca}^{2+}$  ions.  $\text{C}_2\text{O}_4^{2-}$  anions would then be attracted to the  $\text{Ca}^{2+}$ -enriched environment and the crystal nucleus of CaOxa would form. Growth of CaOxa crystals would then be controlled by the cell walls or the biomolecules in the bacterial cells.

Bacteria can produce many extracellular proteins such as enzymes, etc.;<sup>[34]</sup> therefore, we also studied the secretions of *E. coli* in detail by means of zeta potential and FTIR measurements to clarify the interaction between the bacteria and CaOxa. The zeta potential of *E. coli* secretions in aqueous solution shows a peak at about  $-137$  mV (Figure 8), which implies that they are negatively charged and

could therefore strongly attract and enrich  $\text{Ca}^{2+}$  through electrostatic interactions to provide nucleation sites for CaOxa crystals.

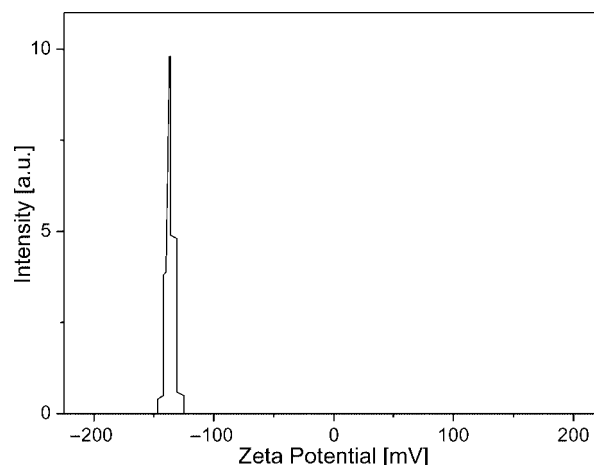


Figure 8. Zeta potential of the *E. coli* secretions in aqueous solution (*E. coli*: 0.5 wt.%).

Figure 9 shows the FTIR spectra of *E. coli* and its secretions in the absence and presence of  $\text{CaCl}_2$ . Figure 9a clearly shows that their principal components are mainly proteins, and the main bands at  $1640$ ,  $1543$ , and  $1401$   $\text{cm}^{-1}$  can be assigned to amide I ( $\nu_{\text{C=O}}$ ), II ( $\delta_{\text{N-H}}$ ), and III ( $\nu_{\text{C-N}}$ ) absorptions, respectively. In the spectrum in Figure 9b, which was recorded in the presence of  $\text{Ca}^{2+}$ , the amide I band is shifted by  $6$   $\text{cm}^{-1}$  to lower frequencies and the amide II band has disappeared, which indicates that there are strong interactions between  $\text{Ca}^{2+}$  ions and the proteins secreted by *E. coli*. In order to obtain more detailed information, the secondary structures of the proteins with and without  $\text{Ca}^{2+}$  ions were studied by recording the second derivative followed by a curve fitting (shown in Figure 10a, b).<sup>[35]</sup> In the absence of  $\text{Ca}^{2+}$  ions, the bands located at  $1641$ ,  $1632$ ,  $1623$ , and  $1614$   $\text{cm}^{-1}$  were assigned to a  $\beta$ -sheet, that at  $1677$   $\text{cm}^{-1}$  to a  $\beta$ -turn, those at  $1669$  and  $1661$   $\text{cm}^{-1}$  to an  $\alpha$ -helix, and that at  $1652$   $\text{cm}^{-1}$  to a random coil of a protein secondary structure. In the presence of  $\text{Ca}^{2+}$  ions, however, the bands attributed to the  $\beta$ -sheet are found at  $1690$ ,  $1641$ ,  $1631$ ,  $1622$ ,  $1613$ , and  $1603$   $\text{cm}^{-1}$ , that for the  $\beta$ -turn at  $1678$   $\text{cm}^{-1}$ , those for the  $\alpha$ -helix at  $1669$  and  $1662$   $\text{cm}^{-1}$ , and that for the random coil at  $1653$   $\text{cm}^{-1}$ . The percentages of  $\beta$ -sheet,  $\beta$ -turn,  $\alpha$ -helix and random coil of *E. coli* proteins in the absence and presence of  $\text{Ca}^{2+}$  ions change from 53.5%, 14.2%, 13.4%, and 18.9% in the former case to 62.4%, 8.8%, 11.3%, and 17.5% in the latter. This indicates that, compared with that of the proteins, the percentage of  $\beta$ -sheet of protein- $\text{Ca}^{2+}$  compounds increases while the percentage of  $\beta$ -turn,  $\alpha$ -helix, and random coil all significantly decreased, which suggests that the interaction between  $\text{Ca}^{2+}$  and proteins makes the conformation of the proteins become more ordered. These ordered proteins could influence the nucleation, growth, and aggregation of CaOxa crystals.

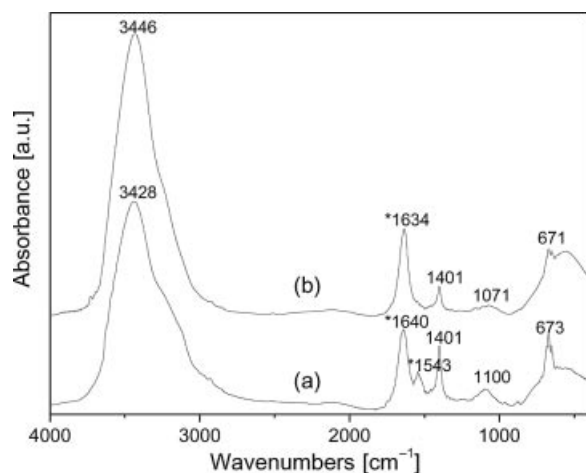


Figure 9. FTIR spectra of (a) *E. coli* aqueous solution (*E. coli*: 0.5 wt.-%) and (b) *E. coli*/CaCl<sub>2</sub> aqueous solution (*E. coli*: 0.5 wt.-%; CaCl<sub>2</sub>:  $5 \times 10^{-3}$  M). The amide I and II bands of the *E. coli* proteins are labeled with an asterisk.

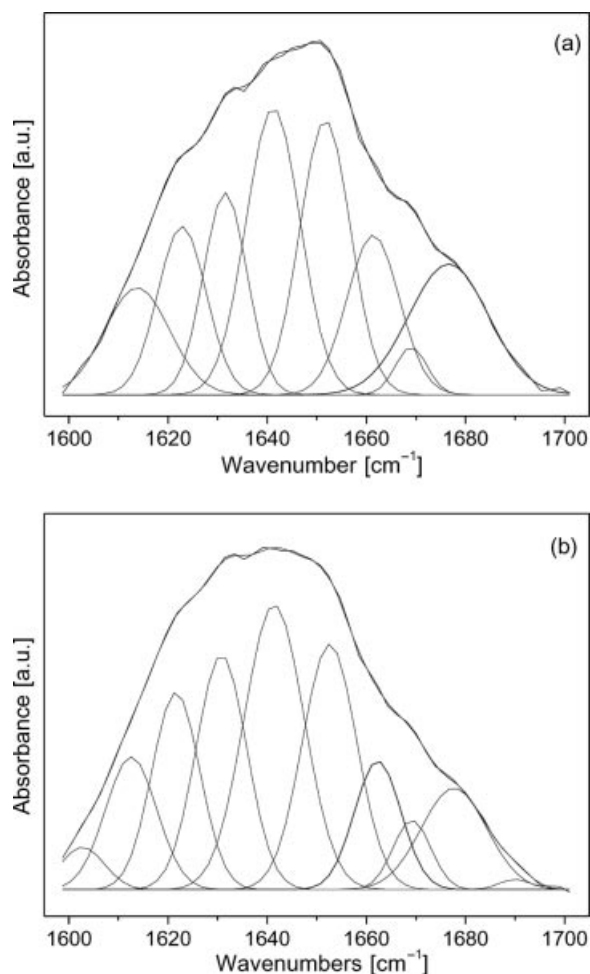


Figure 10. Second derivative and Gaussian curve fitting of the bands between 1600 and 1700 cm<sup>-1</sup> (amide I of proteins) for (a) *E. coli* proteins and (b) *E. coli* protein-Ca<sup>2+</sup> complexes.

According to the Gibbs–Thomson formula of classic nucleation theory,<sup>[36]</sup> the nucleation and growth of CaOxa induced by *E. coli* could be explained by thermodynamic Equation (1), where  $J$  and  $S$  are the nucleation rate and supersaturation, respectively, and  $A$  and  $B$  are constants.

$$J = A \exp[-B(\ln S)^{-2}] \quad (1)$$

We can see from this equation that the rate of nucleation increases with an increase of supersaturation. The interaction between *E. coli* proteins and Ca<sup>2+</sup> ions concentrates these ions around the negatively charged groups of the proteins, which results in an increased supersaturation of CaOxa in this region. As a result, the nucleation rate of CaOxa is increased and the electronegative and ordered proteins also direct the growth of the nucleus and promote the formation of COM crystals. The bacteria therefore accelerate the nucleation and growth of COM crystals.

The above results imply that the common bacterium *E. coli* could also induce the nucleation and growth of CaOxa crystals and accelerate the crystallization of COM when it infects the urinary tract, which means that *E. coli* plays an important role in biomineralization and promotes the formation of urinary stones.

## Conclusions

Investigation of the influence of *E. coli* on the nucleation and growth of CaOxa crystals in aqueous solution has shown that this bacterium accelerates the formation of COM crystals and makes the particles become larger. When the concentration of CaOxa is decreased, the ratio bacteria/CaOxa increases, the COM crystals obtained become more regular and larger, and the phase transition from COD to COM occurs more rapidly. TEM and FTIR results have shown that the nucleation and growth of CaOxa crystals are induced by intracellular biomolecules and bacterial secretions. SDS-PAGE data and UV/Vis spectroscopy have shown that the surface-bound proteins with a molecular weight of about 26.5 kDa contain tyrosine, tryptophan, or phenylalanine residues. The formation mechanism of CaOxa in the presence of *E. coli* has also been discussed. It is likely that the negatively charged *E. coli* proteins interact strongly with Ca<sup>2+</sup> ions and make the secondary structure of these proteins more ordered. These ordered proteins induce the nucleation and growth of CaOxa crystals. *E. coli* is therefore likely to play an important role in biomineralization and promote the formation of urinary stone.

## Experimental Section

**Materials and Instruments:** Chloroform, anhydrous ethanol, and acetone were all purchased from Shanghai Chemical Reagent Company (Shanghai, China) and were all analytically pure. Anhydrous calcium chloride, sodium hydroxide, hydrochloric acid, and sodium oxalate (Na<sub>2</sub>Oxa) were obtained commercially and were also analytically pure. All the above reagents were used without further purification. Doubly distilled water was used in all experiments. Bacteria (*E. coli*) were cultivated on beef peptone culture medium after 48 h incubation at 37 °C in our laboratory. Fourier transform infrared



spectra were recorded with a Nicolet 870 instrument with a resolution of  $4\text{ cm}^{-1}$  in the wavenumber range from 400 to  $4000\text{ cm}^{-1}$  using the KBr pellet technique. X-ray diffraction patterns were recorded with a DX-2000 diffractometer using  $\text{Cu-K}\alpha$  radiation at a scan rate of  $0.06^\circ$  in  $2\theta$  per second. Scanning electron microscopy was performed with a Hitachi X-650 instrument at an accelerating voltage of 20 kV. Transmission electron microscopy and selected-area electron diffraction studies of the CaOxa particles were carried out with a JEM model 100SX electron microscope from Japan Electron Co. at an accelerating voltage at 200 kV. A UV/Vis double beam spectrophotometer (Beijing Purkinje General Instrument Co., Ltd, China) and a zeta potentiometer (Malvern Instruments Limited) were also used.

**Methods:** In a typical experiment, the appropriate amount of *E. coli* was added to a  $5 \times 10^{-2}$  or  $5 \times 10^{-3}\text{ M}$  aqueous solution of  $\text{CaCl}_2$  (40 mL), and this solution was mixed with the same concentration and volume of an aqueous  $\text{Na}_2\text{Oxa}$  solution. The reaction solution was airproofed and kept at a temperature of  $35 \pm 1^\circ\text{C}$  for between 5 min and 72 h after stirring for 30 s. The concentration of *E. coli* in the reaction solution was kept constant at 0.5 wt.-% and the pH of the solution was adjusted to about 7.0. Control experiments were carried out under the same conditions without addition of bacteria. The size and the morphology of the precipitates obtained were examined by scanning electron microscopy (SEM), while their crystalline phases were examined by X-ray powder diffraction (XRD). The zeta potential of an aqueous *E. coli* (0.5 wt.-%) solution was measured to determine the nature of the charge of the bacterial secretions. A drop of an aqueous *E. coli* solution (*E. coli*: 0.5 wt.-%) with and without  $\text{CaCl}_2$  ( $\text{CaCl}_2$ :  $5 \times 10^{-3}\text{ M}$ ) was placed on a KBr crystal after aging for 1 h at a temperature of  $35 \pm 1^\circ\text{C}$  and dried before recording the FTIR spectra to determine the composition of the *E. coli* secretion and the interaction between the *E. coli* secretion and  $\text{Ca}^{2+}$  ions. A drop of reaction solution (*E. coli*: 0.5 wt.-%; CaOxa:  $2.5 \times 10^{-3}\text{ M}$ ) was placed on a copper grid after aging for 12 h at a temperature of  $35 \pm 1^\circ\text{C}$  and dried before recording the TEM image and SAED patterns in order to investigate the influence of the bacterium on the growth of CaOxa crystals. The particles obtained by centrifuging the reaction solution (after aging for 12 h) were washed with doubly distilled water and dried for FTIR spectroscopic determination. To identify the proteins bound to the calcium oxalate crystals that are possibly responsible for the crystal shape and type control, the CaOxa crystals obtained in the presence of bacteria were washed thoroughly after aging for 72 h and then treated with 4% sodium hypochlorite ( $\text{NaOCl}$ ) solution. The free proteins detached from the COM crystals in solution were separated by centrifugation and analyzed by 10% SDS-PAGE at pH = 8.2 and UV/Vis spectroscopy.

## Acknowledgments

This work was supported by the National Science Foundation of China (20471001, 20671001), the Important Project of Anhui Provincial Education Department (ZD2007004-1), and the Specific Project for Talents of Science and Technology of the Universities of Anhui Province (2005 hzbz03).

- [1] S. Atanassova, K. Neykov, I. Gutzow, *J. Cryst. Growth* **2000**, 212, 233–238.
- [2] E. L. Prien, E. L. Prien, *Am. J. Med.* **1968**, 45, 654–672.
- [3] A. Smesko, R. P. Singh, A. C. Lanza-laco, G. H. Nancollas, *Colloids Surf.* **1988**, 30, 361–371.
- [4] S. R. Khan, R. L. Hackett, *J. Urol.* **1993**, 150, 239–245.
- [5] W. H. Boyce, F. K. Garvey, *J. Urol.* **1956**, 76, 213–227.
- [6] S. Whippis, S. R. Khan, F. J. O'Palko, R. Backov, D. R. Talham, *J. Cryst. Growth* **1998**, 192, 243–249.
- [7] R. Backov, S. R. Khan, C. Mingotaud, K. Byer, C. M. Lee, D. R. Talham, *J. Am. Soc. Nephrol.* **1999**, 10, S359–S363.
- [8] R. Backov, C. M. Lee, S. R. Khan, C. Mingotaud, G. E. Fanucci, D. R. Talham, *Langmuir* **2000**, 16, 6013–6019.
- [9] S. R. Khan, P. A. Glenton, R. Backov, D. R. Talham, *Kidney Int.* **2002**, 62, 2062–2072.
- [10] I. O. Benítez, D. R. Talham, *Langmuir* **2004**, 20, 8287–8293.
- [11] I. O. Benítez, D. R. Talham, *J. Am. Chem. Soc.* **2005**, 127, 2814–2815.
- [12] J. M. Ouyang, S. P. Deng, *Dalton Trans.* **2003**, 2846–2851.
- [13] J. M. Ouyang, L. Duan, J. H. He, B. Tieke, *Chem. Lett.* **2003**, 32, 268–269.
- [14] L. J. Wang, S. R. Qiu, W. Zachowicz, X. Y. Guan, J. J. De-Yoreo, G. H. Nancollas, J. R. Hoyer, *Langmuir* **2006**, 22, 7279–7285.
- [15] Y. H. Shen, W. J. Yue, A. J. Xie, S. K. Li, Z. Qian, *Colloids Surf., B* **2005**, 45, 120–124.
- [16] Y. H. Shen, W. J. Yue, A. J. Xie, Z. Q. Lin, F. Z. Huang, *Colloids Surf., A* **2004**, 234, 35–41.
- [17] M. Khullar, S. K. Sharma, S. K. Singh, P. Bajwa, F. A. Sheikh, M. Sharma, *Urol. Res.* **2004**, 32, 190–195.
- [18] N. Ciftcioglu, M. Bjorklund, K. Kuorikoski, K. Bergstrom, E. O. Kajander, *Kidney Int.* **1999**, 56, 1893–1898.
- [19] E. O. Kajander, M. Bjorklund, N. Ciftcioglu, *Proc. SPIE-Int. Soc. Opt. Eng.* **1998**, 3441, 86–94.
- [20] N. Ciftcioglu, M. Bjorklund, E. O. Kajander, *Proc. SPIE-Int. Soc. Opt. Eng.* **1998**, 3441, 105–111.
- [21] E. G. Cuerpo, E. O. Kajander, N. Ciftcioglu, F. L. Castellano, C. Correa, J. Gonzalez, F. Mampaso, F. Liano, E. G. de Gabirola, A. E. Barrilero, *Arch. Esp. Urol.* **2000**, 53, 291–303.
- [22] K. K. Akerman, J. T. Kuikka, N. Ciftcioglu, J. Parkkinen, K. A. Bergstrom, I. Kuronen, E. O. Kajander, *Proc. SPIE-Int. Soc. Opt. Eng.* **1997**, 3111, 436–442.
- [23] F. A. Shiekh, M. Khullar, S. K. Singh, *Urol. Res.* **2006**, 34, 53–57.
- [24] C. Kwak, H. K. Kim, E. C. Kim, M. S. Choi, H. H. Kim, *Eur. Urol.* **2003**, 44, 475–481.
- [25] R. Kumar, M. Mukherjee, M. Bhandari, A. Kumar, H. Sidhu, R. D. Mittal, *Eur. Urol.* **2002**, 41, 318–322.
- [26] A. Edin-Liljegren, L. Grenabo, H. Hedelin, J. Larsson, S. Pettersson, *Scand. J. Urol. Nephrol.* **1993**, 27, 163–167.
- [27] A. Edin-Liljegren, L. Rodin, L. Grenabo, H. Hedelin, *Scand. J. Urol. Nephrol.* **2001**, 35, 106–111.
- [28] N. S. Morris, D. J. Stickler, R. J. McLean, *World J. Urol.* **1999**, 17, 345–350.
- [29] M. Donnet, N. Jongen, J. Lemaitre, P. Bowen, *J. Mater. Sci. Lett.* **2000**, 19, 749–750.
- [30] P. J. du Toit, C. H. van Aswegen, P. L. Steyn, A. Pols, D. J. du Plessis, *Urol. Res.* **1992**, 20, 393–397.
- [31] P. Bassi, *Stone Formation*, in *Handbook of Biom mineralization – Medical and Clinical Aspects* (Eds: M. Epple, E. Bauerlein), Wiley-VCH, Weinheim, Germany, **2007**, pp. 329–348.
- [32] J. K. Lim, N. W. Gunther, H. Zhao, D. E. Johnson, S. K. Keay, H. L. T. Mobley, *Infect. Immun.* **1998**, 66, 3303–3310.
- [33] T. A. Kanellopoulos, P. J. Vassilakos, M. Kantzis, A. Ellina, F. Kolonitsiou, D. A. Papanastasiou, *Eur. J. Pediatr.* **2005**, 164, 355–361.
- [34] G. Butland, J. M. Peregrín-Alvarez, J. Li, W. H. Yang, X. C. Yang, V. Canadien, A. Starostine, D. Richards, B. Beattie, N. Krogan, M. Davey, J. Parkinson, J. Greenblatt, A. Emili, *Nature* **2005**, 433, 531–537.
- [35] A. E. Andreeva, I. R. Karamancheva, *J. Mol. Struct.* **2001**, 565–566, 177–182.
- [36] Y. H. Shen, A. J. Xie, L. C. Huang, F. Z. Huang, Z. X. Chen, D. Ma, *Synth. React. Inorg. Met.-Org. Chem.* **2005**, 35, 359–364.

Received: February 15, 2007  
Published Online: May 29, 2007